www.elsevier.nl/locate/jorganchem

Journal of Organometallic Chemistry 620 (2001) 39–50

Syntheses and structures of doubly tucked-in titanocene complexes with tetramethyl(aryl)cyclopentadienyl ligands

Volkmar Kupfer [a], Ulf Thewalt [a], Iva Tišlerová [b], Petr Štěpnička [c], Róbert Gyepes [c], Jiří Kubišta [d], Michal Horáček [d], Karel Mach [d,*]

[a] *Sektion für Röntgen- und Elektronenbeugung, Universität Ulm, 89069 Ulm, Germany*
[b] *Department of Organic Chemistry, Charles University, Hlavova 2030, 128 40 Prague 2, Czech Republic*
[c] *Department of Inorganic Chemistry, Charles University, Hlavova 2030, 128 40 Prague 2, Czech Republic*
[d] *J. Heyrovský Institute of Physical Chemistry, Academy of Sciences of the Czech Republic, Dolejškova 3, 182 23 Prague 8, Czech Republic*

Received 2 August 2000

Abstract

Titanocene–bis(trimethylsilyl)ethyne complexes [Ti(η^5-$C_5Me_4R)_2$(η^2-$Me_3SiC{\equiv}CSiMe_3$)], where R = benzyl (Bz, **1a**), phenyl (Ph, **1b**) and *p*-fluorophenyl (FPh, **1c**), thermolyse at 150–160°C to give products of double C–H activation [Ti(η^5-C_5Me_4Bz){η^3:η^4-$C_5Me_3(CH_2)(CHPh)$}] (**2a**), [Ti(η^5-C_5Me_4Bz){η^3:η^4-$C_5Me_2Bz(CH_2)_2$}] (**2a′**), [Ti(η^5-C_5Me_4Ph){η^3:η^4-$C_5Me_2Ph(CH_2)_2$}] (**2b**), and [Ti(η^5-C_5Me_4FPh){η^3:η^4-$C_5Me_2FPh(CH_2)_2$}] (**2c**). In the presence of 2,2,7,7-tetramethylocta-3,5-diyne (TMOD) the thermolysis affords analogous doubly tucked-in compounds bearing one η^3:η^4-allyldiene and one η^5-C_5Me_4R ligand having TMOD attached by its C-3 and C-6 carbon atoms to the vicinal methylene groups adjacent to the substituent R (R = Bz (**3a**), Ph (**3b**), and FPh (**3c**)). Compound **3a** is smoothly converted into air-stable titanocene dichloride [$TiCl_2${η^5-$C_5Me_2Bz(CH_2CH(t$-Bu)$CH{=}CHCH(t$-Bu)$CH_2)$}(η^5-C_5Me_4Bz)] (**4a**) by a reaction with hydrogen chloride. Yields in both series of doubly tucked-in complexes decrease in the order of substituents: Bz ≫ Ph > FPh. Crystal structures of **1c**, **2a**, **2b**, and **3b** have been determined.

Keywords: Bis(trimethylsilyl)ethyne complexes; C–H activation; Crystal structures; Diyne cycloaddition; Thermolysis; Titanium; Titanocenes

1. Introduction

Methyl groups in permethylated metallocene derivatives of early transition metals become readily activated under reductive conditions since electron-poor species formed by the reduction tend, in the absence of other ligands, to increase their electron count by oxidative addition of methyl C–H bonds across the electron-deficient metal centre [1]. The transfer of hydrogen from one of the methyl groups to titanium was shown by Bercaw and Brintzinger [2a] to be the main reason of inherent instability of decamethyltitanocene [Ti(η^5-$C_5Me_5)_2$]. Elimination of hydrogen from C–H-activated primary product leads to a singly tucked-in permethyltitanocene [Ti(η^5-C_5Me_5){η^1:η^5-$C_5Me_4(CH_2)$}] [2,3]. Similarly, thermally induced elimination of methane from [TiMe(η^5-$C_5Me_5)_2$] affords the same product, and an elimination of two molecules of methane from [$TiMe_2$(η^5-$C_5Me_5)_2$] gives a doubly tucked-in compound, [Ti(η^5-C_5Me_5){η^3:η^4-$C_5Me_3(CH_2)_2$}] (**2**) [4]. This complex is also obtained by thermolysis of [Ti(η^5-$C_5Me_5)_2$(η^2-$Me_3SiC{\equiv}CSiMe_3$)] (**1**) at 130°C, which, besides complex **2**, affords a mixture of (*E*)- and

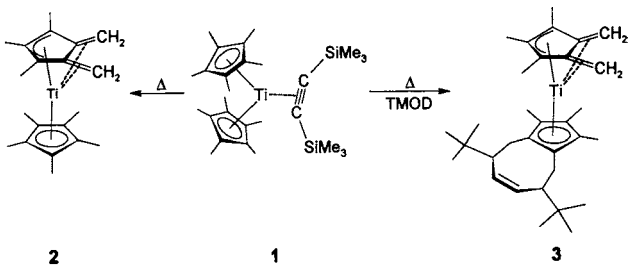

2 1 3

Scheme 1.

* Corresponding author. Tel.: +420-2-8585367; fax: +420-2-8582307.
E-mail address: mach@jh-inst.cas.cz (K. Mach).

0022-328X/01/$ - see front matter
PII: S0022-328X(00)00784-1

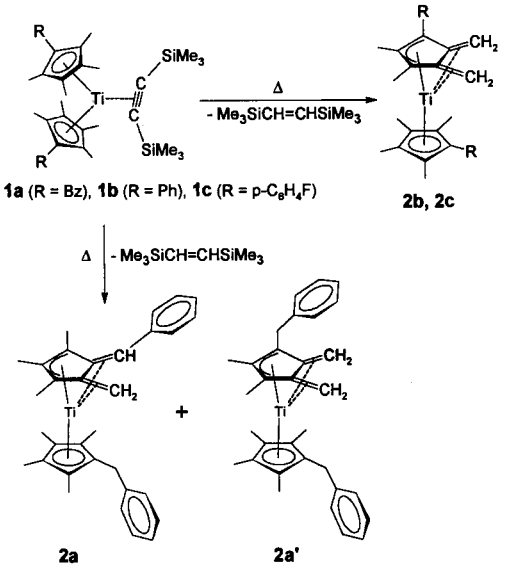

Scheme 2.

(*Z*)-$Me_3SiCH{=}CHSiMe_3$ ($E \gg Z$) as the product of twofold hydrogen transfer from a titanocene intermediate onto the alkyne triple bond (Scheme 1) [5]. Compounds [Ti(η^5-$C_5Me_4R)_2$(η^2-$Me_3SiC{\equiv}CSiMe_3$)], where R = H or $SiMe_3$, behave differently: at 200°C the former gave a mixture of isomeric complexes [Ti(η^5-C_5Me_4H){η^3:η^4-$C_5Me_2(CH_2)_2H$}] in a very low yield [5], whereas the latter afforded titanocene [Ti(η^5-$C_5Me_4(SiMe_3)$}$_2$] in high yield at only 70–80°C [6].

It has been demonstrated that the role of proton acceptor in C–H activation of titanocene methyl groups is not restricted to σ-bonded hydrocarbyls or $Me_3SiC{\equiv}CSiMe_3$. When the thermolysis of **1** is carried out in the presence of 2,2,7,7-tetramethylocta-3,5-diyne (TMOD), an unusual cycloaddition of TMOD to vicinal methyl groups of the η^5-C_5Me_5 ligand takes place to afford complex **3** (Scheme 1), bearing two chirality centres in the annelated ring as the sole detectable product in nearly quantitative yield. Complex [Ti(η^5-$C_5Me_4H)_2$(η^2-$Me_3SiC{\equiv}CSiMe_3$)], similar to the above-mentioned thermolysis in the absence of TMOD, gave under similar conditions only a very low yield of the adduct (**3′**). In its structure, vicinal pairs of two *exo*-methylene groups on the newly formed allyldiene ligand and TMOD-substituted methylene groups on the cyclopentadienyl ring are located in a position adjacent to the unsubstituted ring-carbon atom [7].

Because the nature of the substituent R in the [Ti(η^5-$C_5Me_4R)_2$(η^2-$Me_3SiC{\equiv}CSiMe_3$)] compounds undoubtedly controls the efficiency of their thermolysis, we have undertaken a thermolytic study on a series of such complexes containing benzyl, phenyl and *p*-fluorophenyl as the substituent R both without any additive and in the presence of TMOD.

2. Results and discussion

2.1. Thermolysis *1a–c* in the absence of TMOD

Fully cyclopentadienyl-substituted titanocene dichlorides of the type [$TiCl_2$(η^5-$C_5Me_4R)_2$], where R = $CH_2C_6H_5$ (Bz), C_6H_5 (Ph), and *p*-C_6H_4F (FPh), were reduced by magnesium in the presence of bis(trimethylsilyl)ethyne (BTMSE) to give the corresponding η^2-alkyne complexes [Ti(η^5-$C_5Me_4R)_2$(η^2-BTMSE)] (R = Bz, **1a**, Ph, **1b**, and FPh, **1c**), which were thermolysed with and without addition of TMOD at 150–160°C in *m*-xylene solutions. Heating of complex **1a** to 150°C for 3 h in the absence of TMOD affords a mixture of two doubly tucked-in complexes **2a** and **2a′** (Scheme 2). The complexes were separated on the basis of their different solubilities in hexane and obtained in total 87% isolated yield and ca. 10:1 ratio (**2a**:**2a′**). The volatile residue from the thermolysis contained only the solvent and a mixture of $Me_3SiCH{=}CHSiMe_3$ isomers ($E \gg Z$), indicating a transfer of two hydrogen atoms from the titanocene moiety to the leaving BTMSE. As follows from spectral and structural data, the titanium centre in both complexes is coordinated by one η^3:η^4-allyldiene ligand (henceforth denoted as Ad) [4] and one unchanged η^5-cyclopentadienyl ligand (or Cp′), similar to the product of double C–H activation of permethylated complex [Ti(η^5-$C_5Me_5)_2$(η^2-BTMSE)] [5].

The diene system of the Ad ligand in the major product **2a** is formed from the benzyl group and vicinal methyl group, whereas two vicinal methyl groups adjacent to the benzyl group take part in its formation in the case of minor complex **2a′**. Both compounds are easily distinguishable by ^{13}C chemical shifts of the newly formed sp^2 carbon atoms that appear at δ_C 81.0 (=CH_2) and 90.2 (=*C*HPh) in **2a** but at δ_C 68.19 and 68.29 ppm (both =CH_2) in **2a′**. The latter values are in accordance with the NMR data on the doubly tucked-in complexes obtained by boiling a [$TiCl_2$(η^5-$C_5HMe_4)_2$]–$LiAlH_4$ mixture in toluene [8]: δ_C 67.24 and 69.91 were found for the vicinal methylene carbon atoms adjacent to the ring proton (asymmetric isomer), δ_C 67.04 was observed for vicinal methylene groups remote from the ring proton (symmetrical isomer), and δ_C 67.64 for [Ti(η^5-C_5Me_5){η^3:η^4-$C_5Me_3(CH_2)_2$}] [4,9]. Structures assigned to **2a** and **2a′** are further supported by NOESY spectra, which for **2a′** show peaks due to through-space interactions between =CH_2 protons of the Ad ring and methyl groups of both Cp′ and Ad ligands (δ_H 1.0↔1.74, 1.75, 1.79, 2.44 and 3.55) and signals due to interactions of neighbouring methyl groups of the Ad ring (δ_H 1.06↔1.32). More importantly, cross peaks at δ_H 1.32↔2.44 and δ_H 1.79↔3.55 assign the signals of the benzylic CH_2 protons at δ_H 2.44/2.69 and δ_H 3.55 to Ad and Cp′ rings respectively.

In the case of **2a**, NOESY cross-peaks at δ_H 1.21↔2.26, 1.7↔3.4 and 0.97↔1.10 were observed. NMR data are thus in keeping with single-crystal X-ray analysis of **2a** (Section 2.5).

It is also worth noting that in the ^{1}H-NMR spectra of **2a′** the PhCH_2 protons on the Cp′ ligand are equivalent (A_2 spin system), whereas those of the Ad ligand appear as a doublet of doublets due to an AB spin system ($^2J_{HH} = 15.1$ Hz) with remarkable anisochronicity ($\Delta\nu_{AB}/J_{AB} = 6.7$). On the other hand, benzylic protons in **2a** are observed as an AB spin system with large J value but only small separation of the signals, i.e. only weak satellites due to scalar coupling are observed ($^2J_{HH} = 16.4$ Hz; $\Delta\nu_{AB}/J_{AB} = 0.40$). Spectra of both [$TiCl_2(\eta^5$-$C_5Me_4Bz)_2$] [10] and [$Ti(\eta^5$-$C_5Me_4Bz)_2(\eta^2$-BTMSE)] [11] exhibit only true singlets corresponding to the benzylic A_2 spin systems.

Under similar conditions, compounds **1b** and **1c** gave only low yields of analogous doubly tucked-in compounds **2b** and **2c**. Increasing the thermolysis temperature to 160°C did not improve the yields. The non-equivalence of *exo*-methylene carbon resonances (71.3 and 73.2 ppm for **2b** and 71.3 and 72.7 ppm for **2c**) points to an asymmetric structure similar to **2a′** in both cases. This assumption was further confirmed by X-ray diffraction measurement of **2b** (Section 2.5).

All **2**-type complexes are thermally robust, melt above 100°C and give the molecular ions as the base peaks in their electron impact mass spectra. Their infrared spectra are uninformative with respect to the *exo*-methylene bonds because the C–H and C=C bonds of aryl substituents may hide their features. The $\nu(C_{ring}{=}CH_2)$ (or =CHPh) absorption band, however, is very likely shifted below 1500 cm^{-1}, not interfering with the aromatic ring band at 1600 cm^{-1}. This is compatible with the C–C bond order between one and two, as it is also indicated by the chemical shift of the *exo*-methylene carbon atoms, by the C–C bond distance close to 1.44 Å and the geometry of the Ad ligands (see below). The nature of Ti···$CH_2{=}C_{ring}$ bonding in **2** was suggested by Teuben and coworkers [4] to be of π-type, as already expressed by the term 'allyldiene'. An absence of d^2 electrons in ultraviolet photoelectron spectra of **2** was accounted for by their mixing with empty ligand π-orbitals [12]. The electronic absorption spectra of bis(*exo*-methylene) complexes **2a′**, **2b**, and **2c** display an absorption band at 610 nm. In **2a**, containing the methylene/benzylidene diene system, this band is shifted to 580 nm. Hence, it is obvious that the aryl substituents in compounds **2a**, **2b** and **2c** do not affect the bonding. However, they affect the reactivity of the parent BTMSE complexes; as a result of the substituent effects, the yields of doubly tucked-in complexes decrease roughly with the decreasing electron donation effect of the substituents in the order: Me ≈ Bz ≫ Ph > FPh ≈ H (for Me and H see Ref. [5]).

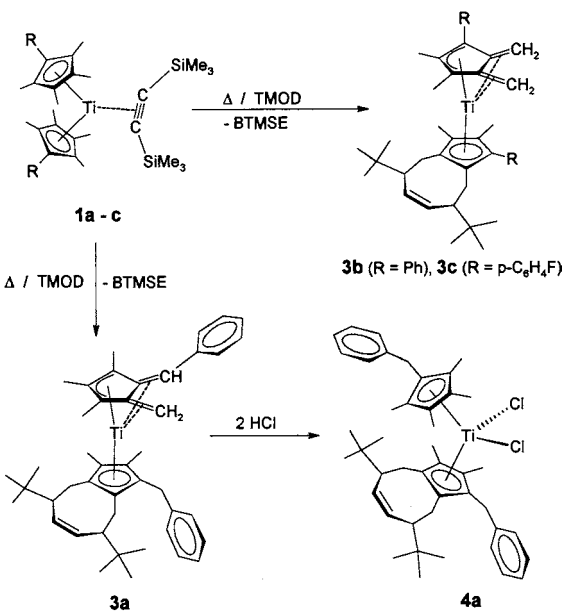

Scheme 3.

2.2. Thermolysis of *1a–c* in the presence of TMOD

Thermolysis of **1a–c** in the presence of TMOD results in the formation of doubly tucked-in compounds **3a–c** with TMOD attached to the C_5Me_4R ligand (Cp′) to give η(1,8-11)-bicyclo[6.3.0]-3,6-bis(2-methyl-2-propyl) - 9,10 - dimethyl - 11 - aryl - undec - 4 - ene - 1(8),9(10)-dien-11-yl (Scheme 3). The cycloaddition of TMOD has apparently no observable influence on the bonding mode of the allyldiene ligands, as indicated by electronic absorption spectra being practically identical with non-annelated analogues **2a–c**, and also the yields of the cycloadducts follow the same order of substituents. The structures of complexes **3a–c** were determined from their NMR spectra and further corroborated by X-ray structural analysis of compound **3b**. The mass spectra show molecular ions as the base peaks, with other intensive signals being due to fragments formed by the loss of the *t*-butyl group and (TMOD + 2H). ^{1}H- and ^{13}C-NMR spectra of complexes **3a–c** clearly identified the structure of the Ad ligands to be identical with the structures of Ad ligands in **2a**, **2b**, and **2c** respectively. A compound analogous to **2a′** was not detected. NMR features due to the annelated octene ring are similar to that of **3** and indicate that the benzyl group is not involved in the ring formation in **3a**. The substitution of the Cp^{TMOD} was not unequivocally determined from the NMR data. However, it is likely that all the **3**-type compounds behave in a uniform manner, forming structures in which the substituent R or proton neighbours the methylene groups of the annelated ring, as observed for the

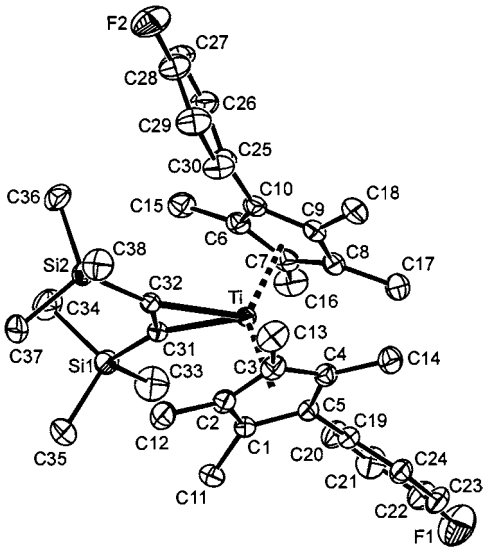

Fig. 1. ORTEP drawing of **1c** with 30% probability ellipsoids and atom numbering scheme.

Table 1
Selected bond lengths (Å) and bond angles (°) for **1c**

Bond distances			
Ti–CE(1)[a]	2.139(2)	Ti–C(31)	2.114(2)
Ti–CE(2)[b]	2.137(2)	Ti–C(32)	2.121(2)
Ti–C(1)	2.418(2)	Ti–C(2)	2.448(2)
Ti–C(3)	2.458(2)	Ti–C(4)	2.507(2)
Ti–C(5)	2.448(2)	Ti–C(6)	2.511(2)
Ti–C(7)	2.484(2)	Ti–C(8)	2.449(2)
Ti–C(10)	2.428(2)	C(31)–C(32)	1.303(3)
C(5)–C(19)	1.480(3)	C(10)–C(25)	1.485(3)
C(22)–F(1)	1.353(3)	C(28)–F(2)	1.360(3)
C(31)–Si(1)	1.860(2)	C(32)–Si(2)	1.874(2)
$(Si(1)–C_{Me})_{av}$	1.874(4)	$(Si(2)–C_{Me})_{av}$	1.875(4)
Bond and dihedral angles			
CE(1)–Ti–CE(2)	138.9(1)	C(31)–Ti–C(32)	35.85(8)
C(31)–C(32)–Ti	71.76(13)	C(32)–C(31)–Ti	72.40(13)
C(31)–C(32)	135.24(18)	C(32)–C(31)	136.35(18)
–Si(2)		–Si(1)	
$\phi(1)$[b]	41.49(12)	$\phi(2)$[c]	19.06(21)
$\phi(3)$[d]	22.47(21)	$\phi(4)$[e]	54.86(10)
$\phi(5)$[f]	48.68(13)		

[a] CE(1): centroid of the Cp′ ring defined by C(1)–C(5) atoms; CE(2): centroid of the Cp′ ring defined by C(6)–C(10) atoms.
[b] Dihedral angle between the least-squares planes defined by the C(1)–C(5) and C(6)–C(10) atoms.
[c] Dihedral angle between the least-squares plane defined by the C(1)–C(5) and the plane defined by the C(31), C(32), and Ti atoms.
[d] Dihedral angle between the least-squares plane defined by the C(6)–C(10) and the plane defined by the C(31), C(32), and Ti atoms.
[e] Dihedral angle between the least-squares planes defined by the C(1)–C(5) and C(19)–C(24) atoms.
[f] Dihedral angle between the least-squares planes defined by the C(6)–C(10) and C(25)–C(30) atoms.

C_5Me_4H analogue **3′** [7] and in the crystal structure of **3b** (vide infra). Hence, the mechanism of the formation of **3a**–**c** can also be expected to be the same as that outlined for compound **3**, requiring a transfer of two pairs of hydrogen atoms from methylene groups of Ad and Cp′ ligands to triple bonds of TMOD [7].

2.3. Derivatization of *3a*

As has been shown recently for compound **3** [13], this highly air-sensitive compound can be converted into an air-stable titanocene dichloride by simply reacting with two equivalents of HCl. This method of derivatization was also shown to be feasible for compound **3a**, which is accessible in high yield. Its hexane solution reacted smoothly with gaseous HCl to give a red finely crystalline titanocene dichloride **4a**, which is stable in air (Scheme 3). Its structure was deduced from mass spectra, ^{1}H- and ^{13}C-NMR spectra and elemental analysis. The mass spectra, although not showing the peaks of the molecular ion, display fragments arising from losses of Cl, Cp′ and Cp^{TMOD} thereof. NMR spectra clearly indicate the replacement of the Ad ligand by the η^5-C_5Me_4Bz ligand, whereas signals due to the Cp^{TMOD} ligand remain.

2.4. Molecular structure of *1c*

The only crystal structure in the series of *p*-fluorophenyl-substituted titanocene derivatives was obtained for the starting compound **1c**. Its molecular structure is shown in Fig. 1 and selected geometrical parameters are given in Table 1. The *p*-fluorophenyl substituents occupy positions vicinal to the hinge positions at the opposite sides of the plane defined by the centroids of the Cp′ rings CE(1) and CE(2) and the titanium atom, as in $[TiCl_2(\eta^5\text{-}C_5Me_4Ph)_2]$ [14]. The values of the CE(1)–Ti–CE(2) angle and the angle between the least-squares planes of the cyclopentadienyl rings are very close to those found in **1** [5,15,16]. Also, within the precision of measurement, the geometry of the η^2-coordinated BTMSE (with the C–C distance close to that of a double bond and the silicon atoms deviated from linear arrangement at an angle of ca. 135°) is identical with those of **1** and similar BTMSE complexes. The carbon atoms of methyl groups in the hinge position of the Cp′ rings show a maximum deviation from the least-squares planes of the Cp′ rings (above 0.3 Å), as is common to structures of analogous complexes [5,6,16]. Other carbon atoms, including the *ipso*-carbon atom of FPh substituents, deviate less. The *p*-fluorophenyl substituents thus probably do not impose a higher steric strain than methyl groups. However, they decrease the overall electron-donating ability of the Cp′ ligand and, hence, affect the reactivity of **1c** compared with that of **1** or other compounds, e.g. $[Ti\{\eta^5\text{-}C_5Me_4(SiMe_3)\}_2(\eta^2\text{-}Me_3SiC{\equiv}CSiMe_3)]$ [6].

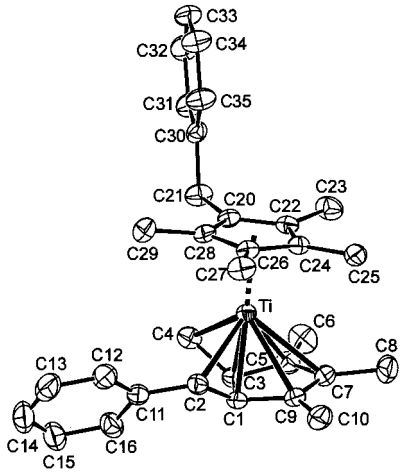

Fig. 2. ORTEP drawing of **2a** with 30% probability ellipsoids and atom numbering scheme.

Table 2
Selected bond lengths (Å) and bond angles (°) for **2a**[a]

Bond distances			
Ti–CE(1)[b]	1.932(4)	C(1)–C(2)	1.438(5)
Ti–CE(2)[c]	1.738(4)	C(1)–C(3)	1.464(5)
Ti–CE(3)[d]	2.026(4)	C(3)–C(4)	1.432(6)
Ti–C(1)	2.086(4)	C(3)–C(5)	1.448(6)
Ti–C(2)	2.298(4)	C(5)–C(7)	1.412(6)
Ti–C(3)	2.072(4)	C(7)–C(9)	1.400(6)
Ti–C(4)	2.228(4)	C(1)–C(9)	1.445(5)
Ti–C(5)	2.364(4)	C(5)–C(6)	1.499(6)
Ti–C(7)	2.522(4)	C(7)–C(8)	1.501(6)
Ti–C(9)	2.347(4)	C(9)–C(10)	1.502(6)
Ti–C(20)	2.343(4)	C(2)–C(11)	1.476(5)
Ti–C(22)	2.350(4)	C(20)–C(21)	1.512(5)
Ti–C(24)	2.356(4)	C(21)–C(30)	1.515(5)
Ti–C(26)	2.375(4)	C_{ring}–$C_{Me}(Cp')_{av}$	1.509(5)
Bond and dihedral angles			
CE(1)–Ti–CE(3)	153.7(2)	C(2)–Ti–C(4)	79.5(2)
Ti–C(2)–C(1)	63.0(2)	Ti–C(4)–C(3)	64.8(2)
C(1)–C(3)–C(5)	107.1(3)	C(3)–C(5)–C(7)	108.1(4)
C(5)–C(7)–C(9)	109.3(4)	C(7)–C(9)–C(1)	109.1(4)
C(1)–C(2)–C(11)	126.6(4)	C(9)–C(1)–C(3)	106.2(3)
C(20)–C(21)–C(30)	114.5(3)	$\phi(1)$[e]	12.4(4)
$\phi(2)$[f]	44.0(4)		

[a] One molecule of *n*-hexane of crystallization is placed in the centre of unit cell: C(36), C(37) and C(38); symmetry operation used to generate equivalent atoms: $(1-x, 1-y, -z)$.

[b] CE(1): centroid of the Cp′ ring defined by atoms C(1), C(3), C(5), C(7) and C(9).

[c] CE(2): centroid of the ring defined by atoms C(1), C(2), C(3) and C(4).

[d] CE(3): centroid of the Cp′ ring defined by atoms C(20), C(22), C(24), C(26) and C(28).

[e] Dihedral angle between the least-squares planes defined by the C(1), C(3), C(5), C(7) and C(9) and C(20)–C(28) atoms.

[f] Dihedral angle between the least-squares planes defined by the C(1), C(3), C(5), C(7) and C(9) and C(1), C(2), C(3) and C(4) atoms.

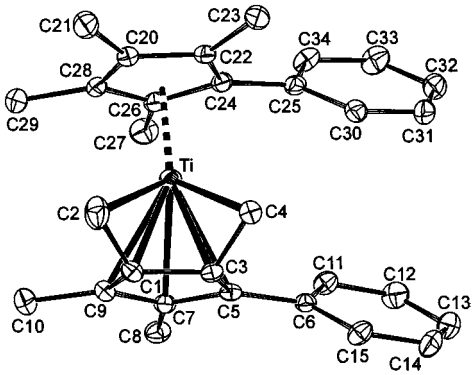

Fig. 3. ORTEP drawing of **2b** with 30% probability ellipsoids and atom numbering scheme.

Table 3
Selected bond lengths (Å) and bond angles (°) for **2b**

Bond distances			
Ti–CE(1)[a]	1.963(3)	C(1)–C(2)	1.439(4)
Ti–CE(2)[b]	1.783(3)	C(1)–C(3)	1.458(4)
Ti–CE(3)[c]	2.047(3)	C(3)–C(4)	1.447(4)
Ti–C(1)	2.117(3)	C(3)–C(5)	1.469(4)
Ti–C(2)	2.316(4)	C(5)–C(7)	1.416(4)
Ti–C(3)	2.107(3)	C(7)–C(9)	1.417(4)
Ti–C(4)	2.252(3)	C(1)–C(9)	1.458(4)
Ti–C(5)	2.381(3)	C(5)–C(6)	1.477(4)
Ti–C(7)	2.550(3)	C(7)–C(8)	1.525(4)
Ti–C(9)	2.389(3)	C(9)–C(10)	1.503(5)
C_{ring}–$C_{Me}(Cp)$	1.514(5)	C(24)–C(25)	1.480(4)
Bond and dihedral angles			
CE(1)–Ti–CE(3)	156.9(1)	C(2)–Ti–C(4)	75.9(1)
Ti–C(2)–C(1)	63.7(2)	Ti–C(4)–C(3)	76.2(2)
C(1)–C(3)–C(5)	106.9(2)	C(3)–C(5)–C(7)	108.7(2)
C(5)–C(7)–C(9)	108.5(2)	C(7)–C(9)–C(1)	109.4(3)
C(7)–C(5)–C(6)	126.3(2)	C(3)–C(5)–C(6)	124.9(2)
C(22)–C(24)–C(25)	125.8(3)	$\phi(1)$[d]	8.3(3)
C(26)–C(24)–C(25)	126.3(2)	$\phi(2)$[e]	43.0(3)

[a] CE(1)-centroid of the Cp′ ring defined by the C(1), C(3), C(5), C(7) and C(9) atoms.

[b] CE(2)-centroid of the ring defined by atoms C(1), C(2), C(3) and C(4).

[c] CE(3)-centroid of the Cp′ ring defined by atoms C(20), C(22), C(24), C(26) and C(28).

[d] Dihedral angle between the least-square planes defined by the C(1), C(3), C(5), C(7), C(9) and C(20), C(22), C(24), C(26) and C(28) atoms.

[e] Dihedral angle between the least-square planes defined by the C(1), C(3), C(5), C(7), C(9) and C(1), C(2), C(3) and C(4) atoms.

2.5. Molecular structures of doubly tucked-in complexes

Molecular structures of **2a**, **2b**, and **3b** commonly contain the central titanium atom bonded to one Ad and one Cp′ ligand; however, they differ in some remarkable features. The Ad ligand in **2a** bears one *exo*-methylene and one benzylidene group in vicinal positions (Fig. 2, Table 2), the structure of **2b** contains two phenyl groups directed into the same direction

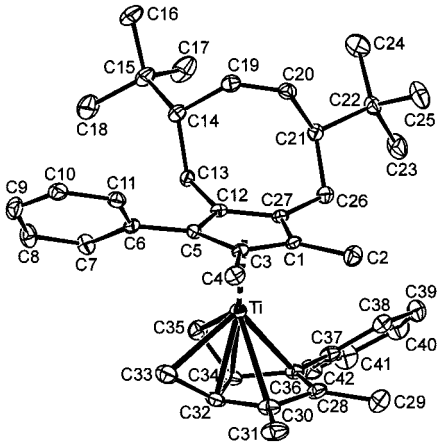

Fig. 4. ORTEP drawing of **3b** with 30% probability ellipsoids and atom numbering scheme.

Table 4
Selected bond lengths (Å) and bond angles (°) for **3b**

Bond distances			
Ti–CE(1)[a]	1.956(4)	C(1)–C(2)	1.504(5)
Ti–CE(2)[b]	1.743(4)	C(1)–C(3)	1.409(5)
Ti–CE(3)[c]	2.029(4)	C(3)–C(4)	1.526(5)
Ti–C(28)	2.561(4)	C(3)–C(5)	1.419(5)
Ti–C(30)	2.382(4)	C(5)–C(6)	1.486(5)
Ti–C(32)	2.081(4)	C(5)–C(12)	1.439(5)
Ti–C(33)	2.257(5)	C(1)–C(9)	1.458(4)
Ti–C(34)	2.088(3)	C(1)–C(27)	1.430(5)
Ti–C(35)	2.234(4)	C(12)–C(27)	1.410(5)
Ti–C(36)	2.376(3)	C(12)–C(13)	1.513(5)
C(32)–C(34)	1.458(5)	C(26)–C(27)	1.522(5)
C(32)–C(33)	1.431(6)	C(19)–C(20)	1.325(6)
C(34)–C(35)	1.434(6)	C(28)–C(29)	1.500(6)
C(34)–C(36)	1.442(6)	C(36)–C(37)	1.498(5)
C(28)–C(36)	1.421(5)	C(30)–C(31)	1.510(5)
C(28)–C(30)	1.409(5)	C(30)–C(32)	1.446(6)
Bond and dihedral angles			
CE(1)–Ti–CE(3)	155.4(2)	C(33)–Ti–C(35)	77.71(19)
Ti–C(33)–C(32)	64.2(2)	Ti–C(35)–C(34)	65.2(2)
C(1)–C(3)–C(5)	106.9(2)	C(28)–C(30)–C(32)	108.8(4)
C(30)–C(32)–C(34)	107.0(4)	C(32)–C(34)–C(36)	106.7(3)
C(34)–C(36)–C(28)	108.9(3)	C(34)–C(36)–C(37)	124.7(3)
C(3)–C(5)–C(6)	126.7(3)	C(5)–C(12)–C(13)	126.0(3)
C(12)–C(27)–C(26)	126.0(3)	C(13)–C(12)–C(27)	125.4(3)
C(14)–C(19)–C(20)	131.2(4)	C(19)–C(20)–C(21)	128.6(4)
$\phi(1)$[d]	9.1(2)	$\phi(2)$[e]	42.9(2)

[a] CE(1)-centroid of the Cp′ ring defined by C(28), C(30), C(32), C(34) and C(36) atoms.

[b] CE(2)-centroid of the ring defined by atoms C(32), C(33), C(34) and C(35).

[c] CE(3)-centroid of the Cp′ ring defined by C(1), C(3), C(5), C(12) and C(27) atoms.

[d] Dihedral angle between the least-square planes defined by the C(28), C(30), C(32), C(34) and C(36) and C(1), C(3), C(5), C(12) and C(27) atoms.

[e] Dihedral angle between the least-square planes defined by the C(28), C(30), C(32), C(34), C(36) and C(32), C(33), C(34) and C(35) atoms.

parallel to each other (Fig. 3, Table 3), and the Cp′ ligand in **3b** is modified by the annelated eight-membered ring arising from the cycloaddition of TMOD (Fig. 4, Table 4). Independently of the various substituents on the cyclopentadienyl ligands (Bz, Ph or Ph/TMOD), the least-squares planes of their rings are perpendicular to the Ti–CE(1) vectors within the precision of the measurements (i.e. no ring slippage is observed). The Ad ligand can be imagined as consisting of two planar systems (or two half-planes): the original cyclopentadienyl ring (now formally the allylic donor system) and a four-membered 1,3-diene π-system. The allyldiene C_5-ring is slipped in such a way that the Ti–C distance increases from the shortest for the carbon atoms common to the both planes (2.072(4)–2.117(3) Å), to the *exo*-methylene carbon atoms 2.228(4)–2,316(4) Å), outer allyl carbon atoms (2.347(4)–2.389(3) Å) and internal allyl carbon atoms (2.522(4)–2.561(4) Å). The distances of the titanium atom from the allyldiene C_5-ring least-squares plane are 1.873(3) Å (**2a**), 1.906(3) Å (**2b**) and 1.889(2) Å (**3b**), and those from the diene least-squares plane are 1.710(4) Å (**2a**), 1.762(3) Å (**2b**) and 1.717(3) Å (**3b**). The angles subtended by these Ad half-planes are 44.0(2)° (**2a**), 43.0(1)° (**2b**) and 42.9(2)° (**3b**). The allyldiene C_5-ring declines from an arrangement parallel to the Cp′ ring plane by an angle of 12.4(2)° for **2a**, 8.3(1)° for **2b** and 9.1(2)° for **3b**, the allyl part of the allyldiene C_5-ring being located at the top of the angle. The deviations of methyl and other carbon atoms attached to the Cp′ and Ad C_5-rings from their least-squares planes are a maximum 0.133(6) Å for C(23) in **2a**, 0.166(5) Å for C(23) in **2b**, and 0.179(6) Å for C(13) and 0.192(6) Å for C(29) in **3b**. The angles between the least-squares planes of the Cp and phenyl rings in **2b** are slightly different, 36.3(2)° and 45.0(2)°, but the difference is approximately equal to the declination of the Cp rings from the parallel arrangement and, hence, the phenyl rings are parallel. The distance between the carbon atoms of these phenyl rings exceeds 4.0 Å, and is larger than the shortest intermolecular distances (ca. 3.7 Å). In **3b**, the dihedral angles of phenyl rings and their adjacent C_5-rings are similar: Cp′/Ph 50.4(1)° and Ad/Ph 34.8(2)°. However, the phenyl rings are placed on opposite sides of the molecule. The geometrical parameters of the Ad ligands, annelated cyclooctene substituent, and common parts of the doubly tucked-in complexes differ only marginally from those of the only known structures of this type in compound **3** and its tetramethyl-substituted analogue **3′** (see Fig. 5) [7]. The bond distances of the *exo*-methylene groups and their adjacent carbon atoms to the titanium centre are essentially the same as those found for the single tucked-in complex $[Ti\{\eta^5{:}\eta^1\text{-}C_5Me_4(CH_2)\}(\eta^5\text{-}C_5Me_5)]$ [17], which is a paramagnetic d^1 system having its *exo*-methylene carbon σ-bonded to titanium [12]. The geometric

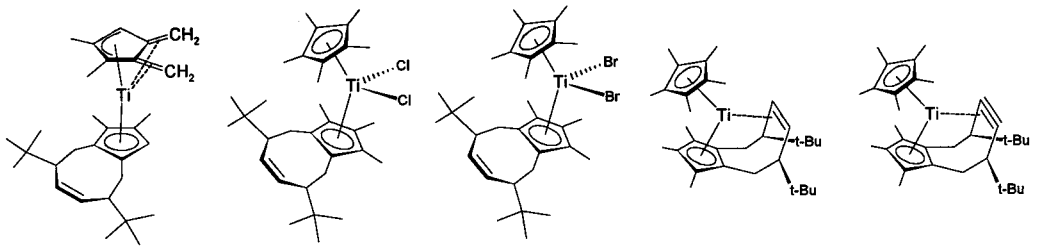

3' 5 5' 6 7

Fig. 5.

Table 5
Ring-puckering coordinates for **3b** and related complexes[a]

Compound	Q_2 (Å)	Q_3 (Å)	Q_4 (Å)	Q (Å)	ϕ_2 (°)	Refs.
3b	1.389(4)	0.066(4)	0.185(4)	1.404(4)	69.3(2)	This work
3	1.262(8)	0.023(8)	−0.219(8)	1.281(8)	335.6(4)	[7]
3′	1.246(3)	0.052(3)	0.284(3)	1.280(3)	168.1(1)	[7]
5	1.342(5)	0.063(5)	0.227(5)	1.362(5)	162.4(2)	[13]
5′	1.347(6)	0.043(7)	−0.231(7)	1.366(6)	343.5(3)	[13]
6	1.449(3)	0.099(3)	0.158(3)	1.461(3)	146.9(1)	[13]
7	1.508(3)	0.066(3)	0.162(3)	1.517(3)	147.7(1)	[13]
$[PdBr_2(\eta^4\text{-}C_8H_{12})]$	1.412(7)	0.019(7)	0.155(7)	1.420(7)	147.0(3)	[19]

[a] See Fig. 5.

parameters, however, seem to be insufficient to extend this conclusion and to suggest σ-Ti–C bonds, and, hence, the Ti(IV) valence, in the doubly tucked-in complexes, too.

Another feature worth mentioning is the conformation of the cyclooctene ring in the structure of **3b**. Table 5 provides a comparison of its ring-puckering coordinates [18] with some related complexes. It is obvious that the conformation of the free eight-membered ring in all the cases mentioned is best described as a twisted boat–boat conformation (ideal values: $Q_2 > 0$, $Q_3 = Q_4 = 0$ and $\phi_2 = k \times 90°$). On the other hand, upon π-coordination of either its central double or triple bond the conformation changes to a boat conformation (ideal values: $Q_2 > 0$, $Q_3 = Q_4 = 0$ and $\phi_2 = k \times 90° + 45°$), similar to that of η^4-coordinated 1,5-cyclooctadiene, for example, as demonstrated by the last entry in Table 5. In this regard, the annelating cyclooctene moiety can be regarded as a rather unique diene system capable of flexible η^4-coordination.

3. Concluding remarks

Substituted analogues of the doubly tucked-in titanocene complex $[Ti(\eta^5\text{-}C_5Me_5)\{\eta^3\text{:}\eta^4\text{-}C_5Me_3(CH_2)_2\}]$ [4,5] can be prepared by thermally induced C–H activation of the complexes $[Ti(\eta^5\text{-}C_5Me_4R)_2(\eta^2\text{-BTMSE})]$ (R = benzyl, phenyl and *p*-fluorophenyl) in the presence and the absence of TMOD. However, their yields decrease strongly in the order of substituents R: Me ≈ Bz ≫ Ph > FPh. The benzyl group takes part preferably in the formation of the allyldiene ligand in the absence of TMOD and exclusively in the presence of TMOD. The cycloaddition of TMOD involves two vicinal methyl groups adjacent to the phenyl group in **3b**; the placement of the annelating cyclooctene ring in a position adjacent to the non-methyl substituent is very likely a common feature of this reaction. It has to be noted that our attempts to carry out analogous cycloadditions of other 1,4-substituted 1,3-butadiynes, e.g. the phenyl and trimethylsilyl derivatives, to the above BTMSE complexes of type **1** were unsuccessful. However, these diynes, as well as TMOD, form a number of products with C–H-activated permethylated titanocenes generated in situ by the reduction of the titanocene dichlorides with magnesium [20,21].

4. Experimental

4.1. General

All manipulations, including spectroscopic measurements, were performed in vacuum using all-sealed glass devices equipped with breakable seals. ^{1}H-(399.95 MHz) and $^{13}C\{^1H\}$-NMR (100.58 MHz) spectra were recorded on a Varian UNITY Inova 400 spectrometer in C_6D_6 solutions at 25°C. Chemical shifts (δ/ppm) are given relative to the solvent signal ($\delta/_H$ 7.15, $\delta/_C$ 128.0). Assignment of the data is based on ^{1}H, $^{13}C\{^1H\}$, ^{13}C-APT, ^{1}H,^{1}H-COSY-90 and ^{13}C-HSQC ex-

periments. NOESY spectra were used to distinguish between isomers **2a** and **2a′**. EI-MS spectra were obtained on a VG-7070E double-focusing mass spectrometer at 70 eV. The crystalline samples in sealed capillaries were opened and inserted into the direct inlet under argon. The spectra are represented by the peaks of relative abundance higher than 6% and by important peaks of lower intensity. GC–MS analyses were performed on a Hewlett Packard gas chromatograph (5890 series II) equipped with a capillary column SPB-1 (length 30 m; Supelco) and a mass spectrometric detector (5971 A). UV–near-IR spectra were measured in the range 280–2000 nm on a Varian Cary 17D spectrometer in all-sealed quartz cuvettes (Hellma). IR spectra were recorded in an air-protecting cuvette on a Specord IR-75 (Carl Zeiss, Jena, Germany) infrared spectrometer. Samples in KBr pellets were prepared in a Labmaster 130 glovebox (mBraun) under purified nitrogen (concentrations of oxygen and water below 2.0 ppm).

4.2. Chemicals

The solvents THF, hexane, and toluene were dried by refluxing over $LiAlH_4$ and stored as solutions of dimeric titanocene $[(\mu\text{-}\eta^5{:}\eta^5\text{-}C_{10}H_8)(\mu\text{-}H)_2\{Ti(\eta^5\text{-}C_5H_5)\}_2]$ [22]. Bis(trimethylsilyl)ethyne (BTMSE, Fluka) was degassed, stored as a solution of dimeric titanocene for 4 h, and finally distilled into ampoules on a vacuum line. 2,2,7,7-Tetramethyl-3,5-octadiyne (TMOD) (Aldrich) was used directly after degassing. Magnesium turnings (Fluka, purum for Grignard reactions) were initially used in large excess for the preparation of $[Ti(\eta^5\text{-}C_5Me_5)_2(\eta^2\text{-BTMSE})]$ [5]. Unreacted highly active magnesium was washed with THF, separated in vacuum and used in subsequent reductions. Compounds **1a** [11], **1b** [11] and $[TiCl_2(\eta^5\text{-}C_5Me_4FPh)_2]$ [10] were prepared by literature procedures.

4.3. Preparation of $[TiCl_2(\eta^5\text{-}C_5Me_4FPh)_2(\eta^2\text{-BTMSE})]$ (1c)

Following the general procedure [23], complex $[TiCl_2(\eta^5\text{-}C_5Me_4FPh)_2]$ (1.0 g, 1.8 mmol) was degassed and mixed with activated magnesium (ca. 0.5 g, 20 mmol), BTMSE (1.0 ml, 4.5 mmol) and THF (40 ml). The mixture was stirred at 60°C until the red colour of the solution turned yellow and then it was heated to 60°C for another 30 min. The resulting yellow solution was separated from unreacted magnesium, THF and BTMSE were distilled off in vacuum and the residue was extracted by 50 ml of hexane. After standing overnight, a grey powder (largely $MgCl_2$) separated from a clear yellow solution. The solution was concentrated and crystallized at ambient temperature to give yellow crystals of **1c**. Yield 1.0 g, 86%. ^{1}H-NMR: δ −0.11 (s, 9H, Me_3Si), 1.77, 1.88 (2 × s, 6H, Me_4C_5); 6.06 (apparent dd, $J' = 5.4$, 8.3 Hz, 2H, C_6H_4F), 6.65 (apparent t, $J' \approx 8.7$ Hz, 2H, C_6H_4F). ^{13}C{^{1}H}-NMR: δ 3.7 (Me_3Si), 13.3 (δ_H 1.77), 14.6 (δ_H 1.88) (Me_4C_5); 114.7 (d, $^2J_{FC} = 21$ Hz, C_6H_4F γ-*C*H), 123.1, 125.2, 125.7 (Me_4C_5, *C*–Me); 130.6 (d, $^3J_{FC} = 7$ Hz, C_6H_4F β-*C*H), 133.7 (d, $^4J_{FC} = 3$ Hz, C_6H_4F α-C_{ipso}), 161.5 (d, $^1J_{FC} = 245$ Hz, C_6H_4F δ-*C*F), 251.6 (η^2-*C*≡*C*). Note: the $^nJ_{FC}$ ($n = 1$–4) agree with those reported for simple monofluorobenzene derivatives *p*-FC_6H_4X [24]. EI-MS (direct inlet, 70 eV, 165°C): complex **1c** dissociates to give *m*/*z* (relative abundance) 478 ($[M - BTMSE]^{+\cdot}$; 9) and fragment ions of BTMSE 170 (5), 157 (9), 156 (18), 155 (100), 73 (20). IR (KBr, cm^{-1}): 3046 (w), 2947 (vs), 2894 (vs), 2853 (sh), 1880 (vw), 1634 (w), 1598 (s), 1560 (s), 1510 (s), 1480 (m), 1440 (m), 1374 (s), 1293 (w), 1240 (vs), 1220 (vs), 1156 (s), 1094 (m), 1014 (m), 988 (w), 832 (vs), 748 (s), 680 (m), 660 (s), 620 (m), 590 (s), 560 (s), 518 (m), 448 (s), 414 (m). UV–near-IR (hexane, 23°C): 400 ≫ 930 nm.

4.4. Thermolysis of complexes 1a–c

m-Xylene (4.0 ml) was added to **1a** (0.64 g, 1.0 mmol) and the solution was heated in a sealed ampoule to 150°C for 3 h, whereupon the initially yellow mixture turned turquoise. All volatiles were distilled off in vacuo and were subjected to GC–MS analysis. The residue was dissolved in 30 ml of warm hexane and left standing overnight to crystallize. A green mother liquor was separated from a turquoise crystalline solid. This solid was dissolved in warm hexane (20 ml) and, after standing overnight, a crystalline solid was separated from the solution. The solid was separated and recrystallized from hexane to give turquoise crystals of **2a** as the major product. The mother liquors were combined, their volumes reduced to 10 ml, and this solution was left to crystallize at ambient temperature. A blue solid crystallized out from a green mother liquor, which was separated and discarded. The blue solid was purified by recrystallization from a minimum amount of warm hexane to give pure **2a′** as a minor product. The volatiles from the thermolysis contained a mixture of (*E*)- and (*Z*)-1,2-bis(trimethylsilyl)ethene and only a trace of BTMSE.

$[Ti(\eta^5\text{-}C_5Me_4Bz)(\eta^3{:}\eta^4\text{-}C_5Me_3(CH_2)(CHPh)]$ (**2a**). Turquoise crystals, yield 0.37 g (79%). M.p. 108°C. ^{1}H-NMR: δ 0.97 (d, 1H, $^2J_{HH} = 4.9$ Hz, AB of =CH_2), 1.08 (s, 3H, *Me*–C), 1.10 (d, 1H, $^2J_{HH} = 4.9$ Hz, AB of =CH_2), 1.21, 1.31, 1.64, 1.65, 1.67, 1.71 (6 × s, 3H, *Me*–C), 2.26 (s, 1H, =C*H*Ph), 3.41 and 3.43 (2 × d, 1H, $^2J_{HH} = 16.4$ Hz, AB of PhCH_2(Cp)), 6.82–7.33 (m, 10H, *Ph*). ^{13}C-NMR (all signals singlets): δ 10.3, 10.7 (2C), 11.5, 11.6, 11.8, 11.9 (7 × *Me*–C), 32.7 (*C*H_2Ph), 81.0 (=*C*H_2), 90.2 (=*C*HPh), 120, 120.2 (2C), 120.3, 122.3, 122.7 (C_{ipso}(Ph), Me–*C*, *C*=CH_2 and/or

C=CHPh), 123.0, 123.9 (*C*H(Ph)), 124.4 (C_{ipso}(Ph), Me–*C*, *C*=CH_2 and/or *C*=CHPh), 126.2, 128.4, 128.7 (*C*H(Ph)), 135.3, 141.3, 143.7, 146.7, 147.2 (C_{ipso}(Ph), Me–*C*, *C*=CH_2 and/or *C*=CHPh). One of the *C*H(Ph) resonances is masked by the solvent signal, (δ_C ca. 128.2) as follows from a comparison of $^{13}C\{^1H\}$- and ^{13}C-APT-NMR spectra. EI-MS (direct inlet, 70 eV, 145°C): *m*/*z* (relative abundance) 470 (15), 469 (41), 468 ($M^{\cdot+}$, 100), 467 (15), 466 (13), 452 (5), 453 (11), 259 (7), 258 (11), 253 (9), 252 (7), 181 (6), 178 (8). IR (KBr, cm^{-1}): 3073 (vw), 3044 (w), 3000 (w), 2890 (m,vb), 2832 (m,b), 1582 (vs,b),1476 (vs,b), 1437 (vs,b), 1372 (s), 1332 (s), 1279 (m), 1260 (w), 1214 (m), 1170 (w), 1150 (vw), 1069 (m), 1023 (s), 993 (w), 927 (w), 897 (w), 887 (m), 839 (m), 823 (m), 794 (m), 760 (s), 724 (vs), 692 (vs), 647 (w), 627 (vw), 612 (w), 592 (vw), 578 (m), 559 (vw), 536 (vw), 517 (s), 455 (w), 440 (m). UV–vis (toluene, nm): 360(sh) ≫ 590.

[Ti(η^5-C_5Me_4Bz)(η^3:η^4-$C_5Me_2Bz(CH_2)_2$)] (**2a′**). Blue crystalline solid, yield 37 mg (8%). M.p. 103°C. ^{1}H-NMR: δ 0.98, 1.00 (2 × d, 1H, $^2J_{HH}$ = 4.7 Hz, AB of =C*H*$_2$); 1.00, 1.01 (2 × d,1H, $^2J_{HH}$ = 4.5 Hz, AB of =C*H*$_2$); 1.06, 1.32 (2 × s, 3H, *Me*–C(Ad)); 1.74, 1.75 (2 × s, 3H, *Me*–C(Cp)); 1.79 (s, 6H, *Me*–C(Cp)); 2.44, 2.69 (2 × d, 1H, $^2J_{HH}$ = 15.1 Hz, AB of PhC*H*$_2$(Ad)); 3.55 (s, 2H, PhC*H*$_2$(Cp)), 7.07–7.53 (m, 10H, *Ph*). ^{13}C-NMR (all signals singlets): δ 10.18, 10.58 (*Me*–C(Ad)); 11.95, 12.31 (*Me*–C(Cp)); 31.06 (Ph*C*H$_2$(Ad)), 33.26 (Ph*C*H$_2$(Cp)), 68.19, 68.29 (=*C*H$_2$); 119.74, 119.76, 120.00, 120.02 (Me–*C*(Cp)); 122.59, 123.81 (Me–*C*(Ad) or C_{ipso}(Ph)); 126.16, 126.34 (*C*H(Ph)); 126.71 (Me–*C*(Ad) or C_{ipso}(Ph)), 128.47, 128.73, 128.75, 128.77 (*C*H(Ph)); 134.01 (Me–*C*(Ad) or C_{ipso}(Ph)), 141.59, 142.01 (CH$_2$–*C*(Cp and Ad)); 144.32, 145.50 (*C*=CH$_2$(Ad)). EI-MS (direct inlet, 70 eV, 145°C): *m*/*z* (relative abundance) 470 (16), 469 (41), 468 (100), 467 (16), 466 (17), 454 (12), 453 (30), 259 (9), 258 (15), 254 (5), 253 (9), 252 (7), 181 (6), 180 (5), 179 (6), 178 (8) 91 (5). There is no remarkable difference between the two isomers in the mass spectra. UV–vis (hexane, nm): 310(sh) ≫ 610.

An analogous thermolysis of **1b** and **1c** and the workup of products afforded blue, poorly crystallizing compounds **2b** and **2c** in moderate and low yield respectively. Repeated attempts to isolate other products from dirty-green hexane mother liquors of the thermolysis failed. Volatiles from thermolytic mixtures contained minor amounts of (*E*)- and (*Z*)-1,2-bis(trimethylsilyl)ethene in addition to major BTMSE.

[Ti(η^5-C_5Me_4Ph){η^3:η^4-$C_5Me_2(C_6H_5)(CH_2)_2$}] (**2b**). Blue crystals, yield 0.15 g (34%). M.p. 124°C. ^{1}H-NMR: δ 1.01, 1.05 (2 × d, 1H, $^2J_{HH}$ = 4.2, =CH$_2$); 1.07 (d, 1H, $^2J_{HH}$ = 4.4, =CH$_2$), 1.13 (*Me*), 1.16 (d, 1H, $^2J_{HH}$ = 4.4, =CH$_2$), 1.54, 1.66, 1.70, 1.85, 1.98 (5 × *Me*); 6.87–7.23 (m, 10H). $^{13}C\{^1H\}$-NMR (all signals are singlets): δ 10.6 (δ_H 1.13), 11.6 (δ_H 1.54), 11.9 (δ_H 1.66), 12.2 (δ_H 1.70), 13.1 (δ_H 1.85), 13.6 (δ_H 1.98) (6 × *Me*); 71.3 (δ_H 1.01 and 1.05), 73.2 (δ_H 1.07 and 1.16) (=*C*H$_2$); 119.3, 119.9, 120.6, 121.2, 124.1 (*C*–Me, *C*–Ph and Ph C_{ipso}); 126.3, 126.4, 128.9, 130.4 (Ph, *C*H; two signals are overlapped by the solvent resonance); 133.4, 135.6, 137.1 (*C*–Me, *C*–Ph and Ph C_{ipso}); 142.9, 146.7 (*C*=CH$_2$). EI-MS (direct inlet, 70 eV, 130°C; *m*/*z* (%)): 442 (15), 441 (43), 440 ($M^{\cdot+}$; 100), 439 (16), 438 (13), 425 ($[M-Me]^+$, 9), 423 (5), 242 ($[M-Cp']^+$, 6), 241 (8), 240 (10), 239 (7), 238 (7), 237 (10), 181 (5), 165 (8), 41 (5). IR (KBr) (cm^{-1}): 3074 (w), 3034 (m), 2966 (s), 2933 (sh), 2900 (vs), 2847 (s), 1596 (s), 1568 (w), 1500 (s), 1474 (m), 1447 (s), 1426 (s), 1366 (s), 1353 (m), 1260 (w), 1214 (vw), 1173 (vw), 1153 (vw), 1093 (w), 1073 (m), 1020 (s), 980 (w), 914 (w), 894 (m), 847 (m), 832 (s), 820 (s), 800 (m), 773 (m), 754 (vs), 724 (s), 700 (vs), 660 (w), 644 (w), 626 (w), 610 (w), 586 (m), 575 (m), 498 (m), 440 (m). UV–vis (hexane, nm): 320(sh) > 390(sh) ≫ 610.

[Ti{η^5-C_5Me_4(*p*-C_6H_4F)}{η^3:η^4-C_5Me_2(*p*-C_6H_4F)-$(CH_2)_2$}] (**2c**). Blue crystals, yield 90 mg (19%). M.p. 123°C. ^{1}H-NMR: δ 0.98, 1.01 (2 × d, 1H, $^2J_{HH}$ = 4.4, =C*H*$_2$ *A*); 1.02 (s, 2H, =C*H*$_2$ *B*), 1.09, 1.44, 1.57, 1.68, 1.73, 1.92 (6 × *Me*); 6.59–6.96 (m, 8H). $^{13}C\{^1H\}$-NMR (singlets if not stated otherwise): δ 10.5 (δ_H 1.09), 11.4 (δ_H 1.44), 11.6 (δ_H 1.57), 12.1 (δ_H 1.68), 13.0 (δ_H 1.73), 13.5 (δ_H 1.92) (6 × *Me*); 71.3 (=*C*H$_2$ *A*), 72.7 (=*C*H$_2$ *B*), 114.8 (d, $^2J_{FC}$ = 21 Hz, C_6H_4F γ-*C*H), 115.0 (d, $^2J_{FC}$ = 22 Hz, C_6H_4F γ-*C*H), 119.0, 120.1, 120.4, 121.2, 124.2, 126.6, 128.9, 129.3 (*C*–Me, *C*–C_6H_4F and C_6H_4F C_{ipso}), 130.4 (d, $^3J_{FC}$ = 7 Hz, C_6H_4F β-*C*H), 131.8 (d, $^3J_{FC}$ = 8 Hz, C_6H_4F β-*C*H), 142.9, 146.7 (*C*=CH$_2$); 161.6, 161.8 (2 × d, $^1J_{FC}$ = 245 Hz, C_6H_4F α-*C*H). EI-MS (direct inlet, 70 eV, 120°C): *m*/*z* (relative abundance) 478 (16), 477 (42), 476 ($M^{+\cdot}$; 100), 475 (17), 474 (13), 461 ($[M-Me]^+$; 8), 260 (9), 259 (8), 258 (7), 165 (7). IR (KBr) (cm^{-1}): 3053 (w), 3037 (w), 2965 (m), 2940 (m), 2904 (s), 2854 (m), 1877 (vw), 1600 (m), 1509 (vs), 1475 (s), 1445 (m,b), 1404 (w), 1375 (s), 1348 (m), 1293 (w), 1260 (w), 1224 (vs), 1156 (s), 1096 (m), 1026 (s), 1015 (s), 900 (m), 843 (s), 825 (vs), 794 (m), 764 (m), 748 (w), 722 (w), 698 (w), 661 (vw), 620 (w), 589 (s), 580 (m), 560 (m), 520 (sh), 514 (s), 467 (m), 435 (m).

*4.5. Thermolysis of complexes **1a–c** in the presence of TMOD*

Compound **1a** (0.64 g, 1.0 mmol) was dissolved in *m*-xylene (4.0 ml) and the solution was added to degassed TMOD (0.17 g, 1.05 mmol). The resulting mixture was heated in a sealed ampoule to 150°C for 3 h. The yellow colour of the solution turned turquoise. All volatiles were distilled off in vacuo and analysed by

GC–MS. The solid residue was twice crystallized by dissolving in warm hexane (15 ml) and allowing the solution to crystallize overnight; a turquoise crystalline solid separated from a green mother liquor. The solid was recrystallized from toluene to give turquoise crystals of **3a** as the only isolated product. The volatiles from the thermolysis contained BTMSE without admixture of hydrogenated products.

[Ti{(η^5 - $C_5Me_2(PhCH_2)(CH_2CH(t$ - Bu)CH=CHCH-(t-Bu)CH_2)}{η^3:η^4-$C_5Me_3(CH_2)(CHPh)$}] (**3a**). Turquoise crystals, yield 0.46 g (73%). M.p. 168°C. ^{1}H-NMR: δ 0.83, 0.86 (2 × s, 9H, $(CH_3)_3C$); 1.03 (d, 1H, $^2J_{HH}$ = 4.7 Hz, =CH_2), 1.18 (s, 3H, CH_3), 1.20 (d, 1H, $^2J_{HH}$ = 4.7 Hz, =CH_2), 1.27, 1.39 (2 × s, 3H, CH_3); 1.63–1.69 (m, 1H, signal overlapped by a methyl resonance), 1.66, 1.74 (2 × s, 3H, CH_3); 2.22 (dd, 1H, $^3J_{HH}$ = 4.8, $^2J_{HH}$ = 15.9 Hz, CH_2 *B*), 2.30 (dd, 1H, $^3J_{HH}$ = 5.5, $^2J_{HH}$ = 13.8 Hz, CH_2 *A*), 2.37 (s, 1H, =C*H*Ph), 2.61 (dd, 1H, $^3J_{HH}$ = 13.0, $^2J_{HH}$ = 15.9 Hz, CH_2 *B*), 2.71 (dd, 1H, $^3J_{HH} \approx {}^2J_{HH} \approx$ 13.8 Hz, CH_2 *A*), 3.01 (ddd, 1H, $^3J_{HH}$ = 4.8, 9.2, 13.0 Hz, C*H B*), 3.38, 3.47 (2 × d, $^2J_{HH}$ = 16.7 Hz, PhCH_2); 5.50 (dd, 1H, $^3J_{HH}$ = 6.6, 12.0 Hz, C*H* = *A*), 5.56 (dd, 1H, $^3J_{HH}$ = 9.2, 12.0 Hz, C*H* = *B*), 6.82–7.37 (m, 10H, *Ph*CH_2). {^{13}C}^{1}H-NMR: δ 10.4 (δ_H 1.18), 10.8 (δ_H 1.27), 10.8 (δ_H 1.39), 11.6 (δ_H 1.66), 12.1 (δ_H 1.74) (5 × CH_3); 27.6 ($(CH_3)_3C$, δ_H 0.86), 27.7 (CH_2 *A*), 28.1 ($(CH_3)_3C$, δ_H 0.83), 29.3 (CH_2 *B*), 32.1 (PhCH_2), 34.1, 34.9 (2 × $(CH_3)_3C$); 45.4 (*C*H *B*), 52.6 (*C*H *A*), 81.0 (=CH_2), 90.2 (=*C*HPh), 120.2, 120.8, 122.3, 122.4 (C_{ipso} of Cp, Ad and Ph rings); 123.0, 123.9 (*C*H(Ph)); 124.3, 124.4, 125.2 (C_{ipso} of Cp, Ad and Ph rings); 126.2, 127.6, 128.4, 128.5 (*C*H(Ph)); 130.8 (*C*H = *A*), 132.0 (*C*H = *B*), 135.3, 142.4, 143.8,146.4, 147.1 (C_{ipso} of Cp, Ad and Ph rings). EI-MS (direct inlet, 70 eV, 155°C): *m*/*z* (relative abundance) 636 (10), 635 (15), 634 (37), 633 (57), 632 ($M^{+\cdot}$; 100), 631 (18), 629 (13), 617 (9), 576 (26), 575 ([M − *t*-Bu]$^+$; 53), 574 (11), 573 (11), 470 (13), 469 (26), 468 ([M − (TMOD + 2H)]$^+$; 55), 467 (11), 466 (10), 454 (7), 453 (16), 258 (20), 257 (20), 256 (8), 254 (11), 252 (24), 251 (15), 250 (8), 249 (10), 180 (12), 179 (9), 178 (10), 177 (13), 91 (15). IR (KBr, cm^{-1}): 3066 (vw), 3050 (w), 3017 (m), 3000 (m), 2941 (vs), 2898 (s), 2858 (s), 1595 (vs), 1493 (vs), 1456 (s), 1391 (m), 1379 (m), 1363 (s), 1336 (m), 1282 (w), 1260 (w), 1218 (m), 1173 (w), 1153 (vw), 1100 (w), 1072 (m), 1027 (s), 891 (w), 841 (w), 826 (m), 796 (m), 762 (m), 733 (s), 701 (vs), 651 (w), 613 (w), 593 (vw), 580 (m), 520 (m), 461 (w), 433 (m). UV–vis (hexane, nm): 580.

[Ti{(η^5 - $C_5Me_2Ph)(CH_2CH(t$ - Bu)CH=CHCH(t - Bu)-CH_2)}{η^3:η^4-$C_5Me_2Ph(CH_2)_2$}] (**3b**). In an analogous experiment, **1b** (0.61 g, 1.0 mmol) and TMOD (0.17 g, 1.05 mmol) in *m*-xylene (4.0 ml) were heated to 150°C for 3 h and then to 160°C for another 3 h to give a green solution. After replacement of all volatiles by hexane, a blue crystalline material separated from a yellowish-green mother liquor. The solid product was recrystallized from a warm hexane to give blue crystals of **3b**. Yield 0.14 g (23%). M.p. 195°C. ^{1}H-NMR: δ 0.80, 0.83 (2 × s, 9H, Me_3C); 0.86 (d, 1H, $^2J_{HH}$ = 3.9 Hz, =CH_2 *A*), 1.18 (s, 3H, *Me*), 1.19 (d, 1H, $^2J_{HH}$ = 3.9 Hz, =CH_2 *A*), 1.20, 1.30 (2 × d, 1H, $^2J_{HH}$ = 4.4 Hz, =CH_2 *B*); 1.67, 1.70, 1.87 (3 × s, 3H, *Me*); 1.90 (dd, 1H, $^3J_{HH}$ = 5.5, $^2J_{HH}$ = 15.6 Hz, CH_2 *A*), 2.03 (ddd, 1H, $^3J_{HH}$ = 4.8, 6.6, 12.8 Hz, C*H B*), 2.44 (dd, 1H, $^3J_{HH}$ = 12.7, $^2J_{HH}$ = 15.6 Hz, CH_2 *A*), 2.83 (dd, 1H, $^3J_{HH} \approx {}^2J_{HH} \approx$ 13.4 Hz, CH_2 *B*), 2.96 (dd, 1H, $^3J_{HH}$ = 4.8, $^2J_{HH}$ = 13.8 Hz, CH_2 *B*), 3.03 (ddd, 1H, $^3J_{HH}$ = 5.5, 9.6, 12.7 Hz, C*H A*), 5.52 (dd, 1H, $^3J_{HH}$ = 9.6, 12.0 Hz, C*H* = *B*), 5.64 (dd, 1H, $^3J_{HH}$ = 6.6, 12.0 Hz, C*H* = *A*), 6.92–7.43 (m, 10H, *Ph*). {^{13}C}^{1}H-NMR: δ 10.7 (δ_H 1.18), 11.9 (δ_H 1.67), 12.3 (δ_H 1.70), 13.4 (δ_H 1.87) (4 × *Me*); 27.5 (Me_3C, δ_H 0.80), 27.5 (CH_2 *A*), 28.1 (Me_3C, δ_H 0.83), 28.8 (CH_2 *B*), 33.1, 34.7 (2 × Me_3C); 45.9 (*C*H *A*), 53.6 (*C*H *B*), 70.8 (=CH_2 *A*), 72.4 (=CH_2 *B*), 120.1, 120.4, 124.2, 124.3, 124.7 (C_{ipso} of Cp, Ad and Ph rings); 126.4, 126.5, 127.9, 128.3, 128.9 (*C*H(Ph)); 129.9 (C_{ipso} of Cp, Ad and Ph rings), 130.9 (*C*H(Ph)); 131.3 (*C*H = *A*), 131.6 (*C*H = *B*), 133.4, 136.0, 137.3, 142.4, 146.7 (C_{ipso} of Cp, Ad and Ph rings). One C_{ipso} signal was not observed. EI-MS (direct inlet, 70 eV, 155°C): *m*/z (relative abundance) 607 (8), 606 (26), 605 (60), 604 ($M^{+\cdot}$; 100), 603 (23), 602 (19), 549 (15), 548 (34), 547 ([M − *t*-Bu]$^+$; 71), 546 (17), 545 (22), 544 (12), 490 (8), 440 (7), 264 (7), 243 (8), 242 (20), 241 (15), 240 (14), 239 (10), 238 (9), 237 (9), 196 (8), 195 (8), 181 (7), 169 (7), 165 (7), 131 (7), 121 (8), 119 (13), 105 (11), 97 (7), 95 (10), 91 (17), 85 (8), 83 (10), 81 (11), 71 (12), 69 (39), 57 (50), 56 (14), 55 (20). IR (KBr, cm^{-1}): 3080 (vw), 3047 (w), 3008 (w), 2950 (vs), 2903 (m), 2861 (m), 1600 (s), 1573 (vw), 1502 (s), 1473 (s), 1466 (s), 1452 (m), 1433 (m), 1392 (m), 1367 (s), 1259 (m), 1227 (m), 1094 (sh,b), 1072 (m), 1022 (s,b), 940 (vw), 911 (w), 896 (vw), 847 (w), 835 (m), 825 (m), 795 (m), 760 (s), 724 (m), 705 (vs), 647 (vw), 631 (vw), 612 (vw), 576 (w), 500 (w), 440 (m). UV–vis (hexane, nm): 390(sh) ≫ 610.

[Ti{(η^5-$C_5Me_2FPh)(CH_2CH(t$-Bu)CH=CHCH(t-Bu)-CH_2)}{η^3:η^4-$C_5Me_2FPh(CH_2)_2$}] (**3c**). Compound **1c** (0.65 g, 1.0 mmol) and TMOD (0.17 g, 1.05 mmol) in *m*-xylene (4.0 ml) were heated to 160°C for 6 h to give a yellow–green solution. After replacement of all volatiles by hexane, a small amount of blue crystalline material separated from a yellowish-green mother liquor. The solid product was recrystallized from a warm toluene to give a blue crystalline **3c**. Yield 50 mg (8%). M.p. 195°C. A very poor solubility of the complex in benzene-d_6 prevented satisfactory recognition and analysis of all the complex ^{1}H-NMR resonances. ^{13}C{^{1}H}-NMR: δ 10.6, 11.8, 12.1, 13.1 (*Me*); 27.4, 28.0 (Me_3C); 27.5, 28.7 (CH_2); 33.1, 34.7 (Me_3C); 45.8, 53.6 (*C*H); 70.8, 72.0 (=CH_2); 131.1, 131.6 (*C*H=*C*H); 115.1,

114.7 (2 × d, $^2J_{FC}$ = 21 Hz, C_6H_4F γ-*C*H); 130.4, 132.4 (2 × $^3J_{FC}$ = 7 Hz C_6H_4F β-*C*H); 142.2, 146.5 (*C*=CH_2); 161.9, 161.9 (2 × d, $^1J_{FC}$ = 245 Hz, C_6H_4F δ-*C*F). Of the ten resonances due to *C*–Me and C_{ipso} C_6H_4F, only four were identified: 119.8, 120.3, 124.3 and 124.9. UV–vis (hexane, nm): 390(sh) ≫ 610.

4.6. Reaction of *3a* with HCl to give *4a*

To a turquoise solution of **3a** (0.27 g, 0.42 mmol) in hexane (30 ml) was admitted excess gaseous HCl [evolved from degassed NaCl (0.10 g, 1.7 mmol) and H_2SO_4 (98%, 5.0 ml)]. The colour turned immediately to red and a brown–red solid precipitated on the walls of the reaction ampoule. After shaking for 1 h, unreacted HCl and about half of the hexane volume were distilled off and the remaining mixture was put into refrigerator overnight. A light-red solution was poured away; the solid was dried in vacuum and dissolved in toluene (10 ml).

[$TiCl_2${η^5-C_5Me_2Bz(CH_2CH(*t*-Bu)CH=CHCH(*t*-Bu)-CH_2)}(η^5-C_5Me_4Bz)] (**4a**). Yield 0.27 g (92%). M.p. 180°C. ^{1}H-NMR: δ 0.91, 1.07 (2 × s, 9H, *Me*$_3$C); 1.88 (s, 3H, *Me*), 1.96 (s, 6H, *Me*), 2.06 (s, 3H, *Me*), 2.09 (s, 6H, *Me*), 1.67 (ddd, 1 H, $^3J_{HH}$ = 5.5, 7.0, 13.6 Hz, C*H A*), 2.46 (dd, 1H, $^3J_{HH}$ = 12.6, $^2J_{HH}$ = 15.8 Hz, CH_2 *B*), 3.02 (dd, 1H, $^3J_{HH}$ = 5.4, $^2J_{HH}$ = 15.8 Hz, CH_2 *B*), 3.05 (dd, 1H, $^3J_{HH}$ = 5.5, $^2J_{HH}$ = 14.3 Hz, CH_2 *A*), 3.39 (ddd, 1H, $^3J_{HH}$ = 5.4, 9.8, 12.6 Hz, C*H B*), 3.52 (dd, 1H, $^3J_{HH} \approx {}^2J_{HH}$ ≈ 14.0 Hz, CH_2 *B*), 4.18 (d, 1H, $^2J_{HH}$ = 17.1 Hz, AB of PhCH_2), 4.20 (s, 2H, PhCH_2), 4.25 (d, 1H, $^2J_{HH}$ = 17.1 Hz, AB of PhCH_2), 5.35 (dd, $^3J_{HH}$ = 7.0, 11.8, =C*H A*), 5.46 (dd, $^3J_{HH}$ = 9.8, 11.8, =C*H B*), 6.91–7.24 (m, 10H, *Ph*CH_2). ^{13}C{^{1}H}-NMR: δ 12.7 (δ_H 1.88), 13.0 (δ_H 1.96), 13.6 (δ_H 2.06), 13.8 (δ_H 2.09) (4 × *Me*); 27.3 (Me_3C), 27.6 (δ_H 1.07, *Me*$_3$C), 27.8 (Me_3C), 28.1 (δ_H 0.91, *Me*$_3$C), 29.8 (*C*H_2 *A*), 30.1 (*C*H_2 *B*), 34.0 (Ph*C*H_2, δ_H 4.20), 34.4 (Ph*C*H_2, δ_H 4.18 and 4.25), 45.3 (*C*H *B*), 51.5 (*C*H *A*), 124.5 (Cp and Ph; C_{ipso}), 126.2 (2C), 128.3, 128.4, 128.5, 128.7 (Ph, *C*H); 129.3, 129.4, 130.2, 130.7 (Cp and Ph; C_{ipso}); 131.0 (*C*H = *A*), 131.4 (*C*H = *B*), 131.7, 132.3, 136.0, 140.7, 141.4 (Cp and Ph; C_{ipso}). EI-MS (direct inlet, 70 eV, 155°C): *m*/*z* (relative abundance) 704 ($M^{+\cdot}$; not observed), 671 (15), 670 (31), 669 $[M-Cl]^+$; 64), 505 (11), 495 (19), 493 ($[M-Cp]^+$; 21), 458 ($[M-Cp-Cl]^+$; 16), 403 (12), 401 ($[M-Cp-Cl-t\text{-Bu}]^+$; 26), 330 (21), 329 ($[M-Cp^{TMOD}]^+$; 38), 328 (19), 296 (38), 295 (34), 294 ($[M-Cp^{TMOD}-Cl]^+$; 100), 293 (30), 292 (15), 212 (20), 211 (42), 210 (21), 209 (17), 119 (51), 91 (76). IR (KBr, cm^{-1}): 3098 (vw), 3075 (w), 3052 (w), 3016 (m), 2998 (m), 2944 (vs), 2897 (s), 2858 (s), 1600 (s), 1580 (w), 1494 (vs), 1474 (s), 1460 (sh), 1450 (vs), 1432 (sh), 1392 (s), 1375 (sh), 1364 (vs), 1283 (w), 1227

Table 6
Crystallographic data, data collection and structure refinement for **1c**, **2a**, **2b** and **3b**[a]

	1c	2a	2b	3b
Chemical formula	$C_{38}H_{50}F_2Si_2Ti$	$C_{32}H_{36}Ti$	$C_{30}H_{32}Ti$	$C_{42}H_{52}Ti$
Molecular weight	648.87	468.52	440.46	604.76
Crystal system	Monoclinic	Triclinic	Monoclinic	Triclinic
Space group	$P2_1/n$ (no. 14)	$P\bar{1}$ (no. 2)	$P2_1/n$ (no. 14)	$P\bar{1}$ (no. 2)
a (Å)	17.4380(4)	8.702(2)	8.7274(14)	10.9192(11)
b (Å)	12.9870(4)	11.580(4)	28.153(3)	11.8159(13)
c (Å)	17.7950(4)	15.055(3)	9.7255(12)	14.9834(14)
α (°)	90.0	91.07(3)	90.0	81.210(12)
β (°)	116.5790(15)	99.549(19)	90.977(15)	87.733(12)
γ (°)	90.0	103.53(4)	90.0	64.220(11)
V (Å^3)	3604.09(16)	1451.9(7)	2389.2(5)	1719.5(3)
Z	4	2	4	2
D_{calc} (g cm^{-3})	1.196	1.170	1.224	1.168
μ (mm^{-1})	0.339	0.315	0.372	0.276
Crystal description	Yellow prism	Turquoise prism	Blue prism	Blue prism
Crystal size (mm^3)	0.5 × 0.4 × 0.3	0.7 × 0.6 × 0.2	0.8 × 0.2 × 0.1	0.46 × 0.38 × 0.19
θ range (°)	2.02–27.49	3.01–25.01	2.22–25.84	1.94–26.00
hkl range	0/22; 0/16; −23/20	−10/10; −13/13; 0/17	−10/9; −34/34; −11/11	−13/13; −14/14; −18/18
Diffractions collected	8183	5482	17 010	9002
Unique diffractions	8183	5096	4341	4570
F(000)	1384	550	936	652
Number of parameters	588	329	280	412
$R(F)$; $wR(F^2)$ (%)	6.94; 14.99	9.85; 16.78	7.63; 13.94	11.36; 10.03
GOF (F^2) all data	1.131	1.193	1.027	0.853
$R(F)$; $wR(F^2)$ [$I>2\sigma(I)$]	4.85; 12.73	6.22; 14.34	5.07; 12.88	4.93; 8.62
Δρ (e$^-$ Å^{-3})	0.303; −0.291	0.277; −0.255	0.673; −0.571	0.244; −0.205

[a] Definitions: $R(F) = \Sigma \|F_o|-|F_c\| / \Sigma |F_o|$, $wR(F^2) = \{\Sigma [w(F_o^2-F_c^2)^2] / [\Sigma w(F_o^2)^2]\}^{1/2}$, GOF = $\{\Sigma [w(F_o^2-F_c^2)^2] / (N_{diffrs}-N_{params})\}^{1/2}$.

(m), 1176 (vw), 1151 (vw), 1107 (vw), 1073 (w), 1029 (s), 1017 (m), 820 (vw), 793 (m), 750 (sh), 732 (s), 699 (vs), 676 (w), 460 (m).

4.7. Crystal structure determination

Fragments of crystals of **1c**, **2a**, **2b** and **3b** were fixed in Lindemann glass capillaries under purified nitrogen in a glovebox and closed with a sealing wax. The X-ray measurements were carried out at room temperature. Diffraction data for **1c** were collected on an Enraf–Nonius CAD-4 MACH III diffractometer, those for **2a** were collected on a Philips PW1100 four-circle diffractometer upgraded by STOE, and those for **2b** and **3b** on a STOE IPDS Imaging Plate System at room temperature using graphite-monochromated Mo–K_α radiation ($\lambda = 0.710\ 73$ Å). The structures of **1c**, **2a** and **2b** were solved by direct methods [25] and that of **3b** by the Patterson method [26]. The structures were refined by full-matrix least-squares methods based on F^2 using a variance-based weighting scheme in the final stages [27]. The non-hydrogen atoms were refined anisotropically. All hydrogen atoms in **1c,** at C(2) in **2a**, and at C(19), C(20), C(33) and C(35) in **3b** were determined from difference Fourier maps and were refined isotropically. All other hydrogen atoms were included at their calculated positions and refined isotropically. Compound **2a** contained one molecule of *n*-hexane of crystallization in the unit cell located on the inversion centre. Crystal data, details of data collection and refinement are given in Table 6.

5. Supplementary material

Crystallographic data, excluding structure factors, have been deposited at the Cambridge Crystallographic Data Centre as supplementary publication nos CCDC-147448 (**1c**), CCDC-144792 (**2a**), CCDC-144793 (**2b**), and CCDC-144794 (**3b**). Copies of the data can be obtained free of charge on application to The Director, CCDC, Union Road, Cambridge CD12 1EZ, UK (fax: +44-1223-336033; e-mail: deposit@ccdc.cam.ac.uk).

Acknowledgements

This work was supported by the Grant Agency of the Czech Republic (project no. 203/99/0846), by the Council for Research and Development of Academy of Sciences of the Czech Republic (project no. S4040017), and by Volkswagen Stiftung.

References

[1] (a) N.J. Long, Metallocenes, Blackwell, Oxford, UK, 1998. (b) R. Beckhaus, in: A. Togni, R.L. Halterman (Eds.), Metallocenes, vol. 1, Wiley–VCH, Weinheim, Germany, 1998, Ch. 4, p. 153.
[2] (a) J.E. Bercaw, H.H. Brintzinger, J. Am. Chem. Soc. 93 (1971) 2046. (b) J.E. Bercaw, R.H. Marvich, L.G. Bell, H.H. Brintzinger, J. Am. Chem. Soc. 94 (1972) 1219. (c) J.E. Bercaw, J. Am. Chem. Soc. 96 (1974) 5087.
[3] J.M. Fischer, W.E. Piers, V.G. Young, Organometallics 15 (1996) 2410.
[4] J.W. Pattiasina, C.E. Hissink, J.L. de Boer, A. Meetsma, J.H. Teuben, A.L. Spek, J. Am. Chem. Soc. 107 (1985) 7758.
[5] V. Varga, K. Mach, M. Polášek, P. Sedmera, J. Hiller, U. Thewalt, S.I. Troyanov, J. Organomet. Chem. 506 (1996) 241.
[6] M. Horáček, V. Kupfer, U. Thewalt, P. Štěpnička, M. Polášek, K. Mach, Organometallics 18 (1999) 3572.
[7] M. Horáček, P. Štěpnička, R. Gyepes, I. Císařová, M. Polášek, K. Mach, P.-M. Pellny, V.V. Burlakov, W. Baumann, A. Spannenberg, U. Rosenthal, J. Am. Chem. Soc. 121 (1999) 10638.
[8] K. Mach, V. Varga, V. Hanuš, P. Sedmera, J. Organomet. Chem. 415 (1991) 87.
[9] R. Beckhaus, J. Sang, J. Oster, T. Wagner, J. Organomet. Chem. 484 (1994) 179.
[10] J. Langmaier, Z. Samec, V. Varga, M. Horáček, K. Mach, J. Organomet. Chem. 579 (1999) 348.
[11] P. Štěpnička, R. Gyepes, I. Císařová, M. Horáček, J. Kubišta, K. Mach, Organometallics 18 (1999) 4869.
[12] T. Vondrák, K. Mach, V. Varga, A. Terpstra, J. Organomet. Chem. 425 (1992) 27.
[13] P.-M. Pellny, V.V. Burlakov, W. Baumann, A. Spannenberg, M. Horáček, P. Štěpnička, K. Mach, U. Rosenthal, Organometallics 19 (2000) 2816.
[14] M. Horáček, M. Polášek, V. Kupfer, U. Thewalt, K. Mach, Collect. Czech Chem. Commun. 64 (1999) 61.
[15] V.V. Burlakov, A.V. Polyakov, A.I. Yanovsky, Yu.T. Struchkov, V.B. Shur, M.E. Vol'pin, U. Rosenthal, H. Görls, J. Organomet. Chem. 476 (1994) 197.
[16] V. Varga, J. Hiller, R. Gyepes, M. Polášek, P. Sedmera, U. Thewalt, K. Mach, J. Organomet. Chem. 538 (1997) 63.
[17] J.M. Fischer, W.E. Piers, V.G. Young, Jr, Organometallics 15 (1996) 2410.
[18] D. Cremer, J.A. Pople, J. Am. Chem. Soc. 97 (1975) 1354.
[19] P. Štěpnička, I. Císařová, Collect. Czech Chem. Commun. 61 (1996) 1335.
[20] P.-M. Pellny, F.G. Kirchbauer, V.V Burlakov, W. Baumann, A. Spannenberg, U. Rosenthal, J. Am. Chem. Soc. 121 (1999) 8313.
[21] P.-M. Pellny, F.G. Kirchbauer, V.V Burlakov, W. Baumann, A. Spannenberg, U. Rosenthal, Chem. Eur. J. 6 (2000) 81.
[22] H. Antropiusová, A. Dosedlová, V. Hanuš, K. Mach, Transition Met. Chem. 6 (1981) 90.
[23] V.V. Burlakov, U. Rosenthal, R. Beckhaus, S.V. Polyakov, Yu.T. Struchkov, G. Oehme, V.B. Shur, M.E. Vol'pin, Metalloorg. Khim. 3 (1990) 476.
[24] V. Wray, in: G.A. Webb (Ed.), Annual Report on NMR Spectroscopy, vol. 14, Academic Press, London, 1983, pp. 251–272.
[25] G.M. Sheldrick, Acta Crystallogr. Sect. A 46 (1990) 467.
[26] G.M. Sheldrick, Z. Dauter, K.S. Wilson, H. Hope, L.C. Sieker, Acta Crystallogr. Sect. D 49 (1993) 18.
[27] G.M. Sheldrick, SHELXS97, Program for Crystal Structure Determination and SHELXL-93, Program for the Refinement of Crystal Structures, University of Göttingen, Germany, 1997.